

Measurements of the Decays $\tau^- \rightarrow h^- h^+ h^- \nu_\tau$ and $\tau^- \rightarrow h^- h^+ h^- \pi^0 \nu_\tau$

R. Balest,¹ K. Cho,¹ W. T. Ford,¹ M. Lohner,¹ H. Park,¹ P. Rankin,¹ J. G. Smith,¹ J. P. Alexander,² C. Bebek,² B. E. Berger,² K. Berkelman,² K. Bloom,² T. E. Browder,^{2,*} D. G. Cassel,² H. A. Cho,² D. M. Coffman,² D. S. Crowcroft,² M. Dickson,² P. S. Drell,² D. J. Dumas,² R. Ehrlich,² R. Elia,² P. Gaidarev,² M. Garcia-Sciveres,² B. Gittelman,² S. W. Gray,² D. L. Hartill,² B. K. Heltsley,² S. Henderson,² C. D. Jones,² S. L. Jones,² J. Kandaswamy,² N. Katayama,² P. C. Kim,² D. L. Kreinick,² T. Lee,² Y. Liu,² G. S. Ludwig,² J. Masui,² J. Mevissen,² N. B. Mistry,² C. R. Ng,² E. Nordberg,² J. R. Patterson,² D. Peterson,² D. Riley,² A. Soffer,² P. Avery,³ A. Freyberger,³ K. Lingel,³ C. Prescott,³ J. Rodriguez,³ S. Yang,³ J. Yelton,³ G. Brandenburg,⁴ D. Cinabro,⁴ T. Liu,⁴ M. Saulnier,⁴ R. Wilson,⁴ H. Yamamoto,⁴ T. Bergfeld,⁵ B. I. Eisenstein,⁵ J. Ernst,⁵ G. E. Gladding,⁵ G. D. Gollin,⁵ M. Palmer,⁵ M. Selen,⁵ J. J. Thaler,⁵ K. W. Edwards,⁶ K. W. McLean,⁶ M. Ogg,⁶ A. Bellerive,⁷ D. I. Britton,⁷ E. R. F. Hyatt,⁷ R. Janicek,⁷ D. B. MacFarlane,⁷ P. M. Patel,⁷ B. Spaan,⁷ A. J. Sadoff,⁸ R. Ammar,⁹ P. Baringer,⁹ A. Bean,⁹ D. Besson,⁹ D. Coppage,⁹ N. Copty,⁹ R. Davis,⁹ N. Hancock,⁹ S. Kotov,⁹ I. Kravchenko,⁹ N. Kwak,⁹ Y. Kubota,¹⁰ M. Lattery,¹⁰ M. Momayezi,¹⁰ J. K. Nelson,¹⁰ S. Patton,¹⁰ R. Poling,¹⁰ V. Savinov,¹⁰ S. Schrenk,¹⁰ R. Wang,¹⁰ M. S. Alam,¹¹ I. J. Kim,¹¹ Z. Ling,¹¹ A. H. Mahmood,¹¹ J. J. O'Neill,¹¹ H. Severini,¹¹ C. R. Sun,¹¹ F. Wappler,¹¹ G. Crawford,¹² R. Fulton,¹² D. Fujino,¹² K. K. Gan,¹² K. Honscheid,¹² H. Kagan,¹² R. Kass,¹² J. Lee,¹² M. Sung,¹² C. White,¹² A. Wolf,¹² M. M. Zoeller,¹² X. Fu,¹³ B. Nemati,¹³ W. R. Ross,¹³ P. Skubic,¹³ M. Wood,¹³ M. Bishai,¹⁴ J. Fast,¹⁴ E. Gerndt,¹⁴ J. W. Hinson,¹⁴ T. Miao,¹⁴ D. H. Miller,¹⁴ M. Modesitt,¹⁴ E. I. Shibata,¹⁴ I. P. J. Shipsey,¹⁴ P. N. Wang,¹⁴ L. Gibbons,¹⁵ S. D. Johnson,¹⁵ Y. Kwon,¹⁵ S. Roberts,¹⁵ E. H. Thorndike,¹⁵ T. E. Coan,¹⁶ J. Dominick,¹⁶ V. Fadeyev,¹⁶ I. Korolkov,¹⁶ M. Lambrecht,¹⁶ S. Sanghera,¹⁶ V. Shelkov,¹⁶ T. Skwarnicki,¹⁶ R. Stroynowski,¹⁶ I. Volobouev,¹⁶ G. Wei,¹⁶ M. Artuso,¹⁷ M. Gao,¹⁷ M. Goldberg,¹⁷ D. He,¹⁷ N. Horwitz,¹⁷ S. Kopp,¹⁷ G. C. Moneti,¹⁷ R. Mountain,¹⁷ F. Muheim,¹⁷ Y. Mukhin,¹⁷ S. Playfer,¹⁷ S. Stone,¹⁷ X. Xing,¹⁷ J. Bartelt,¹⁸ S. E. Csorna,¹⁸ V. Jain,¹⁸ S. Marka,¹⁸ D. Gibaut,¹⁹ K. Kinoshita,¹⁹ P. Pomianowski,¹⁹ B. Barish,²⁰ M. Chadha,²⁰ S. Chan,²⁰ D. F. Cowen,²⁰ G. Eigen,²⁰ J. S. Miller,²⁰ C. O'Grady,²⁰ J. Urheim,²⁰ A. J. Weinstein,²⁰ F. Würthwein,²⁰ D. M. Asner,²¹ M. Athanas,²¹ D. W. Bliss,²¹ W. S. Brower,²¹ G. Masek,²¹ H. P. Paar,²¹ J. Gronberg,²² C. M. Korte,²² R. Kutschke,²² S. Menary,²² R. J. Morrison,²² S. Nakanishi,²² H. N. Nelson,²² T. K. Nelson,²² C. Qiao,²² J. D. Richman,²² D. Roberts,²² A. Ryd,²² H. Tajima,²² and M. S. Witherell²²

(CLEO Collaboration)

¹University of Colorado, Boulder, Colorado 80309-0390

²Cornell University, Ithaca, New York 14853

³University of Florida, Gainesville, Florida 32611

⁴Harvard University, Cambridge, Massachusetts 02138

⁵University of Illinois, Champaign-Urbana, Illinois 61801

⁶Carleton University, Ottawa, Ontario, Canada K1S 5B6

and the Institute of Particle Physics, Montréal, Canada

⁷McGill University, Montréal, Québec, Canada H3A 2T8

and the Institute of Particle Physics, Montréal, Canada

⁸Ithaca College, Ithaca, New York 14850

⁹University of Kansas, Lawrence, Kansas 66045

¹⁰University of Minnesota, Minneapolis, Minnesota 55455

¹¹State University of New York at Albany, Albany, New York 12222

¹²The Ohio State University, Columbus, Ohio 43210

¹³University of Oklahoma, Norman, Oklahoma 73019

¹⁴Purdue University, West Lafayette, Indiana 47907

¹⁵University of Rochester, Rochester, New York 14627

¹⁶Southern Methodist University, Dallas, Texas 75275

¹⁷Syracuse University, Syracuse, New York 13244

¹⁸Vanderbilt University, Nashville, Tennessee 37235

¹⁹Virginia Polytechnic Institute and State University, Blacksburg, Virginia 24061

²⁰California Institute of Technology, Pasadena, California 91125

²¹University of California, San Diego, La Jolla, California 92093

²²University of California, Santa Barbara, California 93106

(Received 14 July 1995)

We use a data sample of 2.8×10^6 produced τ -pair events, obtained with the CLEO II detector, to measure $\mathcal{B}(\tau^- \rightarrow h^- h^+ h^- (\pi^0) \nu_\tau)$, where h refers to either a charged π or K . These branching fractions are measured with samples of lepton-tagged and 3 vs 3 events. We find $\mathcal{B}(\tau^- \rightarrow h^- h^+ h^- \nu_\tau) = 0.0951 \pm 0.0007 \pm 0.0020$ and $\mathcal{B}(\tau^- \rightarrow h^- h^+ h^- \pi^0 \nu_\tau) = 0.0423 \pm 0.0006 \pm 0.0022$. We also measure $\mathcal{B}(\tau^- \rightarrow \omega h^- \nu_\tau) = 0.0195 \pm 0.0007 \pm 0.0011$.

PACS numbers: 13.35.Dx, 14.60.Fg

During the past few years, a consistent picture of tau decays has emerged, particularly for decays to a single charged particle; however, discrepancies remain among measurements with three charged particles in the final state. In particular, there is a large variation among previous measurements of $\mathcal{B}(\tau \rightarrow 3h^\pm \nu_\tau)$, where h refers to either a π or K ; results range from 0.06 to 0.10, with uncertainties less than 0.01 [1]. This decay is dominated by $\tau \rightarrow 3\pi^\pm \nu_\tau$, proceeding predominantly through the a_1 resonance [1]. The branching fraction of the charged a_1 is constrained by isospin to be the same (except for small phase-space corrections) for the $3\pi^\pm$ and $\pi^\pm 2\pi^0$ decay modes. A precise test of the equivalence of these two modes tests these expectations.

Though previous measurements of $\mathcal{B}(\tau \rightarrow 3h^\pm \pi^0 \nu_\tau)$ have been in reasonable agreement, they are not very precise. Most of these used photon counting rather than π^0 reconstruction and thus are more sensitive to unexpected feed-across backgrounds, such as the recently measured $\tau \rightarrow 3h 2\pi^0 \nu_\tau$ decay mode [2]. Since the $\tau \rightarrow 3h \pi^0 \nu_\tau$ mode proceeds through the vector current, $e^+ e^- \rightarrow 4\pi$ data and the conserved-vector-current (CVC) hypothesis have been used to predict a branching fraction for this decay [3,4]. The fraction of the 4π state that proceeds through $\omega\pi$ also has been predicted with CVC [4].

We employ two methods to measure the branching fractions $\mathcal{B}(\tau \rightarrow 3h^\pm \nu_\tau)$ and $\mathcal{B}(\tau \rightarrow 3h^\pm \pi^0 \nu_\tau)$, using tau pairs produced in the reaction $e^+ e^- \rightarrow \tau^+ \tau^-$. In the first method, we select a sample, denoted ℓ -3h (ℓ -3h π^0), in which one τ is required to decay via $\tau \rightarrow \ell \nu$ and the other via $\tau \rightarrow 3h^\pm \nu_\tau$ ($\tau \rightarrow 3h^\pm \pi^0 \nu_\tau$). This method has the advantage that the background from $q\bar{q}$ events ($e^+ e^- \rightarrow q\bar{q}$, $q = udc$) is quite low. In the second approach, we select events in which both τ 's decay to three charged tracks, with the samples denoted 3h-3h and 3h-3h π^0 . The method for the 3h-3h analysis has not been used previously and is possible only with a very large data sample. There are two main advantages: many systematic errors are reduced by a factor of 2 since one measures the square of the branching fraction; and the technique is independent of direct knowledge of any other τ decay modes. We measure $\mathcal{B}(\tau \rightarrow 3h^\pm \pi^0 \nu_\tau)$ with the 3h-3h π^0 sample, since the sample with π^0 's in both hemispheres is small.

The data used in this analysis have been collected with the CLEO II detector [5], operating at a center-of-mass energy, $E_{\text{c.m.}} \approx 10.6$ GeV at the $e^+ e^-$ Cornell Electron Storage Ring. The total integrated luminosity of the sample is 3.0 fb^{-1} , corresponding to 2.8×10^6

τ pairs. CLEO II is a general purpose spectrometer. Showers are reconstructed from energy deposited in a 7800 crystal CsI(Tl) calorimeter, and charged particles are measured with three cylindrical drift chambers inside a 1.5 T superconducting solenoidal magnet. Electrons are identified from specific-ionization (dE/dx) information from the main drift chamber and energy deposited in the calorimeter. Muons are identified with proportional-tube muon chambers embedded in the magnet return iron.

Events are selected for the ℓ -3h (3h-3h) analysis by requiring four (six) charged tracks. The event is divided into hemispheres by the charged-particle thrust axis; leptons are required to be at least 90° from each of the three-prong tracks. The net charge in each hemisphere is required to be ± 1 , and the total charge of the event must be zero. For each track, we require the polar angle θ to lie in the central region of the detector, $|\cos\theta| < 0.81$, and the momentum to be greater than $0.05E_b$, where E_b is the beam energy. To suppress secondary decays such as $K_S \rightarrow \pi\pi$, we veto events if there are any tracks that miss the interaction point by more than 15 mm in the plane normal to the beams. We reject events if an identified electron, when paired with another track, is consistent with arising from a photon conversion.

We suppress $q\bar{q}$ background and feed across from other τ decay modes by vetoing events with calorimeter showers that have energy greater than 100 MeV, are more than 30 cm from the nearest hadronic charged track, and have a lateral profile consistent with that of photons. Events containing showers with energy greater than 800 MeV are rejected regardless of the shower location and shape. For the ℓ -3h (3h-3h) analysis, background from $q\bar{q}$ events is reduced further by requiring 3π invariant masses to be less than 1.777 (1.50) GeV. We remove contamination to the ℓ -3h sample from radiative μ -pair and Bhabha events with a photon conversion by vetoing events for which the scalar sum of the momenta of the three hadron tracks exceeds $0.95E_b$. To reject two-photon background, we require that the polar angle of the missing momentum satisfy $|\cos\theta_{\text{miss}}| < 0.90$ (0.98) for the ℓ -3h (3h-3h) sample, and for the 3h-3h analysis we require the scalar sum of the momenta of the six tracks to be at least $0.45E_{\text{c.m.}}$.

The requirements for the 3h π^0 analyses are the same except for the following: we omit the last three mentioned above, since QED backgrounds are insignificant; for the 3h-3h π^0 analysis we make a 3π (4π) mass cut of 1.5 (1.7) GeV; the energetic-shower veto is applied only after forming π^0 candidates. These π^0 candidates are formed from the two most energetic photons with energy greater

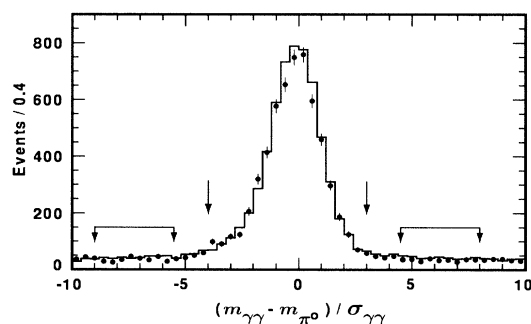


FIG. 1. Normalized mass of π^0 candidates for the ℓ - $3h\pi^0$ analysis. Points are data and histogram is MC. Signal and sideband regions are indicated by arrows.

than 50 MeV and $|\cos\theta| < 0.71$. In Fig. 1 we show the normalized deviation from the π^0 mass for π^0 candidates from the ℓ - $3h\pi^0$ analysis. This quantity, in contrast with $m_{\gamma\gamma}$ itself, is independent of the energy of the photons. We select π^0 's and statistically remove fake π^0 's by using the signal and sideband regions indicated in the figure.

Tagging leptons must satisfy $|\cos\theta| < 0.71$, $p_e > 0.10E_b$, and $p_\mu > 0.26E_b$. Muons are required to penetrate at least 3 interaction lengths of iron and electrons to have dE/dx within 2σ of the expected value and $E_{sh}/p > 0.85$, where E_{sh} is the energy of the calorimeter shower matched to the track. The lepton-identification efficiency is measured with radiative Bhabha and μ -pair events. The hadron-misidentification probabilities are measured with independent τ data samples. Based on this, we determine that the final $3h$ ($3h\pi^0$) sample contains $(0.35 \pm 0.03)\%$ [$(0.44 \pm 0.06)\%$] fake tag electrons and $(4.5 \pm 0.1)\%$ [$(4.4 \pm 0.3)\%$] fake muons.

To determine the efficiencies of the analyses and to estimate the amount of τ feed across and non- τ backgrounds, we have generated samples of τ pair, $q\bar{q}$, and $Y(4S)$ using Monte Carlo (MC) techniques. For τ pairs we use the KORALB generator [6], for $q\bar{q}$ events the Lund generator [7], and for $Y(4S)$ events the CLEO QQ generator [8], which is appropriate for threshold production. The GEANT code [9] is used to simulate the detector response.

We find agreement between data and MC for all variables that are used in the analyses. The 3π masses for the two analyses are shown in Fig. 2, with MC histograms normalized to the measured branching fractions.

In Table I we summarize information for each analysis: the number of data events (N_d), the fraction of τ (f_b^τ) and non- τ ($f_b^{q\bar{q}}$) backgrounds, and the efficiency (ϵ). Errors in the backgrounds and efficiency include systematic errors as discussed below.

For the $3h$ - $3h$ ($3h$ - $3h\pi^0$) analysis, we estimate the amount of $q\bar{q}$ background from MC, scaled by 1.2 ± 0.2 (1.1 ± 0.1) to agree with data in regions where $q\bar{q}$ background dominates. We estimate two-photon background from distributions sensitive to this background and $Y(4S)$ background from MC and find that both are negligible.

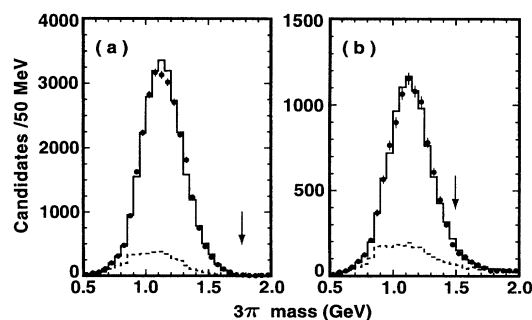


FIG. 2. The mass for $3h$ candidates, assuming $m_h = m_\pi$, for (a) the ℓ - $3h$ analysis; and (b) the $3h$ - $3h$ analysis (2 entries/event). We show data (points with error bars), signal plus background MC (solid line), and background MC (dashed line). Arrows indicate the location of cuts.

For the lepton-tag analysis, we find that $q\bar{q}$ backgrounds are small, as is evident from the region above m_τ in Fig. 2(a), and all other non- τ backgrounds are negligible.

The largest backgrounds are from feed across of other τ decays, which we calculate with our measured branching fractions and those from a recent review [10]. Feed across is dominated by modes with an extra π^0 : $3h\pi^0$ and $3h2\pi^0$, depending on analysis and tag method. Uncertainties in f_b^τ are estimated by comparing MC and data in regions where feed-across background is large. The lepton fake contributions are included in the feed-across background.

We calculate branching fractions from

$$\mathcal{B}_{3h(\pi^0)} = \frac{N_d(1 - f_b^{q\bar{q}} - f_b^\tau)}{2\sigma_{\tau\tau} \mathcal{L} \epsilon \mathcal{B}_\ell} [\ell\text{-}3h(\pi^0)],$$

$$\mathcal{B}_{3h}^2 = \frac{N_d(1 - f_b^{q\bar{q}} - f_b^\tau)}{\sigma_{\tau\tau} \mathcal{L} \epsilon} (3h\text{-}3h),$$

$$\mathcal{B}_{3h\pi^0} = \frac{N_d(1 - f_b^{q\bar{q}} - f_b^\tau)}{2\sigma_{\tau\tau} \mathcal{L} \epsilon \mathcal{B}_{3h}} (3h\text{-}3h\pi^0),$$

where $\sigma_{\tau\tau}$ is the radiatively corrected τ -pair cross section and \mathcal{L} the integrated luminosity. We determine $\sigma_{\tau\tau}$ and \mathcal{L} , each with a precision of 1%, by using, respectively, KORALB, and events from the processes $e^+e^- \rightarrow e^+e^-$, $e^+e^- \rightarrow \gamma\gamma$, and $e^+e^- \rightarrow \mu^+\mu^-$ [11]. For the leptonic branching fractions, \mathcal{B}_ℓ , we use world averages from Ref. [12]. Branching fraction results are given in Table II.

TABLE I. Summary of the numbers of observed events, background fractions, and efficiencies.

Sample	N_d	f_b^τ (%)	$f_b^{q\bar{q}}$ (%)	ϵ (%)
e - $3h$	18 815	7.5 ± 0.2	0.2 ± 0.2	20.0 ± 0.4
μ - $3h$	13 985	12.8 ± 0.2	0.3 ± 0.3	14.4 ± 0.3
$3h$ - $3h$	4877	16.8 ± 1.3	6.5 ± 1.3	14.8 ± 0.4
e - $3h\pi^0$	3227	4.5 ± 0.4	0.3 ± 0.3	7.9 ± 0.3
μ - $3h\pi^0$	2335	10.3 ± 0.4	0.7 ± 0.7	5.6 ± 0.2
$3h$ - $3h\pi^0$	1681	13.6 ± 0.6	12.3 ± 1.4	5.4 ± 0.6

TABLE II. Summary of branching fraction measurements.

Sample	$\mathcal{B}(\tau \rightarrow 3h^\pm \nu_\tau)$	$\mathcal{B}(\tau \rightarrow 3h^\pm \pi^0 \nu_\tau)$
e -tag	$0.0951 \pm 0.0008 \pm 0.0029$	$0.0424 \pm 0.0008 \pm 0.0021$
μ -tag	$0.0948 \pm 0.0008 \pm 0.0031$	$0.0417 \pm 0.0010 \pm 0.0021$
3-3	$0.0952 \pm 0.0009 \pm 0.0021$	$0.0439 \pm 0.0017 \pm 0.0033$
Combined	$0.0951 \pm 0.0007 \pm 0.0020$	$0.0423 \pm 0.0006 \pm 0.0022$

We have considered many contributions to the systematic errors, as summarized in Table III. Uncertainty in the absolute tracking efficiency is estimated by studying a sample of events with a lepton and at least two additional tracks. These are predominantly ℓ - $3h(\pi^0)$ events. We successfully reconstruct the fourth track in 97% of the events, but the reconstruction efficiency is smaller in the MC than in the data by $(0.4 \pm 0.2)\%$. We correct for this difference, though we conservatively assign a systematic error of 0.4%/track, since the origin of the difference is not fully understood. The τ -background systematic error includes uncertainty in the branching fractions of feed-across modes and also the $K\pi\pi$ and $KK\pi$ signal since ϵ is $\sim 15\%$ larger for these modes. Uncertainty in ϵ is determined by varying all selection criteria and adding in quadrature estimates of the individual variations. The uncertainty in π^0 reconstruction efficiency is found by variation of the π^0 criteria and includes uncertainty in the probability for photon conversions.

To determine the combined results, shown in Table II, we form a weighted average, where the weights are calculated from the statistical and systematic errors, taking into account correlations. The correlated systematic errors are typically somewhat larger than the uncorrelated errors. The weights are 0.24 (0.76) for the combined ℓ - $3h$ ($3h$ - $3h$) measurement and 0.88 (0.12) for the ℓ - $3h\pi^0$ ($3h$ - $3h\pi^0$) analysis.

We also explore the spectral function [13] and the $\omega\pi$ component of the $3h\pi^0$ final state, where interference with the $\rho\pi\pi$ components is relatively unimportant. In Fig. 3(a), we plot the mass of the two $\pi^+\pi^-\pi^0$ combinations for the ℓ - $3h\pi^0$ sample. The solid curve is a fit to the data with a MC signal shape and a quadratic background

function. From the fit result of 2223 ± 74 signal events, we find the fraction of all $3h\pi^0$ decays that come from an ωh final state to be $0.412 \pm 0.014 \pm 0.015$. The systematic error comprises 2% from uncertainties in the spectral function and 3% from variations of the fitting method, including uncertainties in the Breit-Wigner shape used in KORALB. Most other systematic errors cancel in this ratio. Using the ℓ - $3h\pi^0$ result for $\mathcal{B}(\tau \rightarrow 3h^\pm \pi^0 \nu_\tau)$ from Table II and accounting for $\mathcal{B}(\omega \rightarrow \pi^+\pi^-\pi^0)$ [1], we find $\mathcal{B}(\tau \rightarrow \omega h \nu_\tau) = 0.0195 \pm 0.0007 \pm 0.0011$. This result is in agreement with, but considerably more precise than, previous measurements [1], and also in agreement with the CVC prediction, 0.0179 ± 0.0014 [4]. In Fig. 3(b), for the $3h\pi^0$ final state and the ωh component, we show data histograms of the spectral function

$$v(m) = \frac{m_\tau^8}{12\pi|V_{ud}|^2} \frac{1}{F(m)} \frac{\mathcal{B}_{3h\pi^0}}{\mathcal{B}_e} \frac{1}{N} \frac{dN}{dm},$$

where m is the 4π mass, $F(m) = m(m_\tau^2 - m^2)^2(m_\tau^2 + 2m^2)$, the quark-mixing matrix element V_{ud} is taken from Ref. [1], and dN/dm is the background-corrected and efficiency-corrected mass distribution for the data. Also shown in this figure are the spectral functions derived from $e^+e^- \rightarrow 4\pi$ data (see Ref. [4]). The agreement between our measurements and this e^+e^- data is good, as expected from CVC, except above 1.4 GeV for the ωh component. The CVC data in this region are dominated by measurements from the DM2 Collaboration [14].

In conclusion, we have measured

$$\begin{aligned} \mathcal{B}(\tau \rightarrow 3h^\pm \nu_\tau) &= 0.0951 \pm 0.0007 \pm 0.0020, \\ \mathcal{B}(\tau \rightarrow 3h^\pm \pi^0 \nu_\tau) &= 0.0423 \pm 0.0006 \pm 0.0022. \end{aligned}$$

TABLE III. Fractional systematic errors for the measured \mathcal{B} 's (%).

Source	$3h$			$3h\pi^0$		
	e -tag	μ -tag	3-3	e -tag	μ -tag	3-3 π^0
Luminosity	1.0	1.0	0.5	1.0	1.0	1.0
Tau cross section	1.0	1.0	0.5	1.0	1.0	1.0
Tracking efficiency	1.6	1.6	1.2	1.6	1.6	1.2
Non- τ backgrounds	0.6	0.4	0.7	0.4	0.8	2.0
τ backgrounds	0.2	0.2	0.8	0.4	0.4	0.8
Efficiency	2.2	2.2	1.3	3.3	3.3	5.6
MC statistics	0.4	0.5	0.4	1.0	1.2	1.5
Lepton ID	0.2	0.8	...	0.2	0.8	...
Tag \mathcal{B}	0.5	0.5	...	0.5	0.5	2.3
π^0 reconstruction	3.0	3.0	3.0
Total	3.1	3.3	2.2	5.0	5.2	7.1

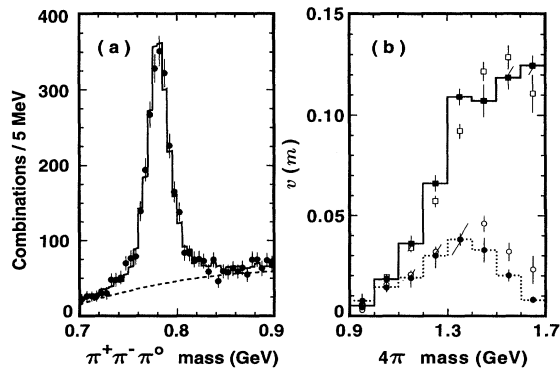


FIG. 3. (a) Invariant mass of $\pi^+\pi^-\pi^0$ combinations (2 entries/event) with the fit (solid histogram) to a MC ω signal shape and quadratic background function (dashed curve). (b) Calculated spectral function for the $3h\pi^0$ final state (open squares) along with the $\omega\pi$ component (open circles). The corresponding spectral functions derived from low-energy e^+e^- data are shown with solid and dashed histograms, respectively.

The measurement for the $3h$ decay is larger, by 4.0 standard deviations, than that in a recent ARGUS publication [15], but in agreement with recent reports from LEP [16]. Subtracting the $K\pi\pi$ and $KK\pi$ modes [10] from this result yields 0.0891 ± 0.0024 , in good agreement with the world average for $\tau \rightarrow \pi 2\pi^0 \nu_\tau$, 0.0909 ± 0.0014 . Our measurement for the $3h\pi^0$ decay is more precise and smaller than previous measurements but in good agreement with the CVC prediction, 0.042 ± 0.003 [4]. Since our data indicate that decays with more than two π^0 's are negligible, we determine the total three-prong branching fraction to be $B_3 = 0.1422 \pm 0.0010 \pm 0.0037$, by combining these $3h$ and $3h\pi^0$ measurements with the CLEO measurement for the $\tau \rightarrow 3h^\pm 2\pi^0 \nu_\tau$ decay [2]. All results in this paper exclude contributions from known decay modes involving K^0 mesons and assume that decays not included in Ref. [10] are negligible. This value of B_3 is in good agreement with other recent measurements and the world average, $B_3 = 0.1432 \pm 0.0027$ [1].

We gratefully acknowledge the effort of the CESR staff in providing us with excellent luminosity and running conditions. We thank K. Hayes and S. Eidelman for many useful discussions. This work was supported by the National Science Foundation, the U.S. Department of Energy, the Heisenberg Foundation, the Alexander von Humboldt Stiftung, the Natural Sciences and Engineering Research Council of Canada, and the A.P. Sloan Foundation.

*Permanent address: University of Hawaii at Manoa, Honolulu, HI 96801.

- [1] Particle Data Group, L. Montanet *et al.*, Phys. Rev. D **50**, 1173 (1994).
- [2] CLEO Collaboration, D. Bortoletto *et al.*, Phys. Rev. Lett. **71**, 1791 (1993).
- [3] F. J. Gilman and S. H. Rhie, Phys. Rev. D **31**, 1066 (1985).
- [4] S. I. Eidelman and V. N. Ivanchenko, Nucl. Phys. B Proc. Suppl. **40**, 131 (1995).
- [5] CLEO Collaboration, Y. Kubota *et al.*, Nucl. Instrum. Methods Phys. Res., Sect. A **320**, 66 (1992).
- [6] KORALB (v.2.2)/TAUOLA (v.2.4): S. Jadach and Z. Was, Comput. Phys. Commun. **64**, 267 (1991); S. Jadach, J. H. Kühn, and Z. Was, *ibid.* **76**, 361 (1993).
- [7] JETSET 7.3: T. Sjöstrand and M. Bengtsson, Comput. Phys. Commun. **43**, 367 (1987).
- [8] P. Avery, K. Read, and G. Trahern, CLEO internal note CSN-212.
- [9] GEANT 3.15: R. Brun *et al.*, Report No. CERN DD/EE/84-1.
- [10] B. K. Heltsley, Nucl. Phys. B Proc. Suppl. **40**, 413 (1995).
- [11] CLEO Collaboration, G. Crawford *et al.*, Nucl. Instrum. Methods Phys. Res., Sect. A **345**, 429 (1994).
- [12] M. Davier, Nucl. Phys. B Proc. Suppl. **40**, 395 (1995); $\mathcal{B}_e = 0.1779 \pm 0.0010$ and $\mathcal{B}_\mu = 0.1733 \pm 0.0010$.
- [13] Y. S. Tsai, Phys. Rev. D **4**, 2821 (1971).
- [14] D. Bisello *et al.*, Report No. LAL 90-35, 1990.
- [15] ARGUS Collaboration, H. Albrecht *et al.*, Z. Phys. C **58**, 61 (1993).
- [16] ALEPH Collaboration, M. Girone *et al.*, Nucl. Phys. B Proc. Suppl. **40**, 153 (1995); OPAL Collaboration, Report No. CERN-PPE/95-070.